 

PACS numbers: 42.55.Px; 42.60.Jf
DOI: 10.1070/QE2009v039n09ABEH014067

# Diode-pumped two-frequency lasers based on *c*-cut vanadate crystals*

A.A. Sirotkin, S.V. Garnov, A.I. Zagumennyi, Yu.D. Zavartsev, S.A. Kutovoi, V.I. Vlasov, I.A. Scherbakov

***Abstract*. The luminescent and lasing properties of the neodymium ion at the $^4F_{3/2} - {}^4I_{11/2}$ transition in *c*-cut vanadate crystals ($Nd:YVO_4$, $Nd:GdVO_4$, and $Nd:Gd_{1-x}Y_xVO_4$) are studied. Tuning of the laser radiation wavelength ($\Delta\lambda = 5.4$ nm) is demonstrated. Two-frequency laser schemes with the use of a Lyot filter, a Fabry – Perot etalon, and a Brewster prism as spectral selection elements are proposed and experimentally realised. Stable two-frequency lasing of a laser based on the *c*-cut $Nd:GdVO_4$ crystal was obtained in the cw, *Q*-switched (nanosecond pulses), and active acousto-optic mode-locked (picosecond pulses) regimes.**

***Keywords***: *two-frequency lasers, diode pumping, vanadate crystals*

## 1. Introduction

The terahertz wavelength region lies between the microwave and far-IR regions. It is a rather interesting informative spectral region for various substances, such as solids, liquids, and biological objects. Terahertz radiation is successfully used in spectroscopy [1 – 3] and biomedicine [4], for analysing proteins and DNA [5], and in safety systems [6, 7]. This radiation has no ionising ability and, hence, the use of harmless terahertz sources instead of X-ray systems can considerably change the situation in the market of diagnostic medical equipment. Terahertz radiation can find application for continuous monitoring of living objects. At present, the works on designing and improving terahertz radiation sources are continued in different directions.

Despite the successful use of femtosecond laser pulses for generating terahertz radiation in a wide frequency region (from tens and hundreds of gigahertz to tens of terahertz), such sources have not yet found wide practical application mainly due to a high cost of femtosecond lasers.

A promising and rapidly developing method to obtain terahertz radiation is to create two-frequency solid-state laser systems generating the difference frequency in photoconducting antennas [8, 9] or nonlinear optical crystals [10, 11]. The method of using two lasers to obtain a difference frequency in the terahertz region has already been used previously [6, 7]. However, the use of two independent lasers creates some problems because it is necessary to match their parameters. A simpler solution is to use laser systems in which the radiation at two wavelengths is generated by one and the same laser rather than by two different lasers. In this case, there is no need to match the laser beams in time and space, owing to which the system can be more compact and reliable. Such approaches were demonstrated using a Ti : sapphire laser [12], diode lasers [13, 14], and a diode-pumped Nd : LSB laser [8]. In the future, this should lead to the creation of less expensive, compact, and frequency-tunable sources of terahertz radiation.

Of practical interest for creating two-frequency solid-state lasers is the search for highly efficient broadband laser crystals, as well as the realisation of tunable two-frequency lasing in the cw, nanosecond, and picosecond regimes. This will allow one to develop sources of terahertz radiation with tunable pulse duration, frequency, and spectral composition (spectral width). The two-frequency nanosecond and picosecond laser pulses can be more efficiently converted in terahertz emitters and nonlinear optical crystals, which makes it possible to increase the output terahertz power.

Today, the active media based on the yttrium ($Nd:YVO_4$), gadolinium ($Nd:GdVO_4$), and mixed ($Nd:Gd_{1-x}Y_xVO_4$) vanadate crystals find the widest application in various diode-pumped lasers due to the optimum combination of their spectroscopic, lasing, and thermal properties. Most researchers use vanadate crystals cut along the *a* axis because the stimu-lated emission and absorption cross sections in this case are maximal. As far as we know, there is only one application of *c*-cut vanadate crystals – in passively *Q*-switched lasers with a $Cr^{4+}$:YAG saturable absorber [15, 16].

However, we showed [17] that the above-listed *c*-cut vanadate crystals are efficient laser media with a broadband luminescence, which can be used for creating frequency-tunable and two-frequency lasers.

## 2. Investigations of the luminescent and lasing properties of active media

In this work, we experimentally studied the luminescent and lasing properties of yttrium ($Nd:YVO_4$), gadolinium ($Nd:GdVO_4$), and mixed ($Nd:Gd_{1-x}Y_xVO_4$) vanadate crystals cut along the *c* axis in order to design efficient

* Reported at the Conference 'Laser optics 2008', St. Petersburg, Russia.

**A.A. Sirotkin, S.V. Garnov, A.I. Zagumennyi, Yu.D. Zavartsev, S.A. Kutovoi, V.I. Vlasov, I.A. Scherbakov** A.M. Prokhorov General Physics Institute, Russian Academy of Sciences, ul. Vavilova 38, 119991 Moscow, Russia; e-mail: saa@kapella.gpi.ru

Received 2 February 2009; revision received 15 April 2009
*Kvantovaya Elektronika* **39** (9) 802 – 806 (2009)
Translated by M.N. Basieva

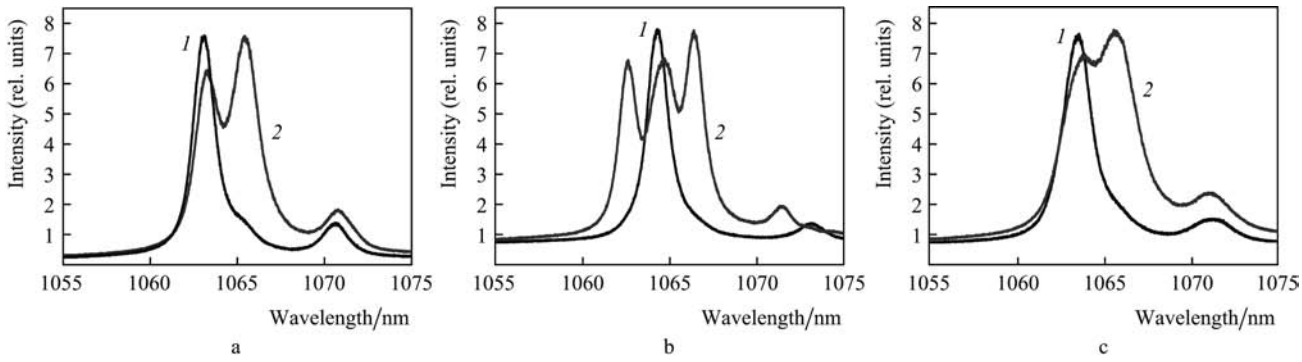


**Figure 1.** Fragments of the luminescence spectra at the $^4F_{3/2}-{}^4I_{9/2}$ laser transition in the (a) $Nd:GdVO_4$, (b) $Nd:YVO_4$, and (c) $Nd:Gd_{0.7}Y_{0.3}VO_4$ crystals cut along the (*1*) *a* and (*2*) *c* axes. The maximum intensities in the spectra of each crystal were taken to be identical.

diode-pumped frequency-tunable and two-frequency lasers based on the $^4F_{3/2}-{}^4I_{11/2}$ transition of neodymium ions in these crystals. The crystals were grown by the Czochralski technique at the General Physics Institute, RAS.

The spectroscopic characteristics of laser crystals were studied using an UV-3101PC (Shimadzu) spectrophotometer and a spectrometer based on a UF-90 autocollimation tube (with the reciprocal linear dispersion 0.1 nm $mm^{-1}$) with a TCD130JK (Toshiba) linear multichannel photodetector.

Figure 1 shows the fragments of luminescence spectra at the $^4F_{3/2}-{}^4I_{11/2}$ transition of the neodymium ion in the $Nd:YVO_4$, $Nd:GdVO_4$, and $Nd:Gd_{0.7}Y_{0.3}VO_4$ crystals cut along the *a* and *c* axes (hereinafter, for the *a*-cut crystals we consider only the $\pi$-polarised radiation). One can see that these spectra are considerably different. The spectral peaks are shifted and the intensity ratios of the inter-Stark transitions are changed. The spectra of the *c*-cut $Nd:GdVO_4$ and $Nd:Gd_{0.7}Y_{0.3}VO_4$ crystals consist of two overlapping lines (the half-widths of the total luminescence profiles are 4.5 and 4.1 nm, respectively). The *c*-cut $Nd:YVO_4$ crystal exhibits three overlapped spectral lines. In this case, the half-width of the total profile is 5.4 nm. The wavelengths of laser radiation and the half-widths of luminescence lines for vanadates cut along the *a* and *c* axes are listed in Table 1.

**Table 1.** Laser radiation wavelengths $\lambda$ and luminescence line half-widths $\Delta\lambda$ for vanadates cut along the *a* and *c* axes.

| Crystal | $\lambda$/nm | | $\Delta\lambda$/nm | |
|---|---|---|---|---|
| | axis *c* | axis *a* | axis *c* | axis *a* |
| $Nd:GdVO_4$ | 1065.5 | 1063.2 | 4.5 | 1.4 |
| $Nd:YVO_4$ | 1066.1 | 1064.1 | 5.4 | 1.0 |
| $Nd:Gd_{0.7}Y_{0.3}VO_4$ | 1065.4 | 1063 | 5.1 | 1.6 |

The intensity and shape of the luminescence line in the mixed vanadate depend on the concentration ratio *x* of Y and Gd. A change in *x* leads to a transformation of the luminescence line profile in the wavelength region of 1062–1066 nm. The broad luminescence lines and the typical two- or three-peak shape of luminescence spectra allow one to use the *c*-cut vanadate crystals for development of efficient frequency-tunable and two-frequency lasers.

## 3. Tuning of laser radiation

The operation efficiencies of lasers based on vanadate crystals cut along the *a* and *c* axes are comparable. However, since the stimulated transition cross sections for the *c*-cut $Nd:GdVO_4$ crystal are considerably smaller than for the *a*-cut crystal, the lasing thresholds for these crystals are different. For example, the lasing threshold for the *c*-cut $Nd:GdVO_4$ crystals was 1.45 W, while the lasing threshold for the *a*-cut crystals was 0.46 W. The conversion efficiency (the ratio of the output laser power to the absorbed pump power) in the $Nd:GdVO_4$ crystals cut along the *a* and *c* axes was 41% and 33% with the slope efficiency of 43% and 41.5%, respectively. Lasing in a nonselective cavity occurs at a wavelength corresponding to the gain maximum, because of which, as follows from Fig. 1a, the laser based on the *c*-cut $Nd:GdVO_4$ crystal operates at a wavelength of 1065.5 nm compared to the laser based on the *a*-cut crystal, whose wavelength is 1063.2 nm. The $Nd:YVO_4$ crystals (Fig. 1b) cut along the *c* and *a* axes operate at wavelengths of 1066.1 and 1064.1 nm, respectively. The lasing wavelength of the *c*-cut $Nd:Gd_{0.7}Y_{0.3}VO_4$ crystal is 1065.4 nm. The overlap of the luminescence lines (Fig. 1) makes it possible to achieve continuous tuning of laser radiation within the total gain profile.

The scheme of the laser setup used to demonstrate the capabilities of laser wavelength tuning is shown in Fig. 2a. As active laser elements, we used the *a*- and *c*-cut $Nd:GdVO_4$, $Nd:YVO_4$, and $Nd:Gd_{0.7}Y_{0.3}VO_4$ crystals $4\times4\times6$ or $4\times4\times8$ mm in size with an atomic neodymium concentration of 0.5 %. The laser crystal was mounted in a water-cooled copper block. The crystal was pumped by a fibre-coupled (core diameter 200 μm, numerical aperture NA = 0.22) HLU30F200 (LIMO) diode system with the maximum output power of 30 W. The pump radiation was focused in the active element into a spot 250–400 mm in diameter.

The laser cavity was formed by a spherical highly reflecting mirror (with a dielectric coating with a high reflectivity at the wavelength of 1064 nm and a high transmittance at the pump wavelength 808 nm) and a plane (transmittance $T = 4.8$ % and 8 %) or spherical (curvature radius 100 mm, $T = 5$ % and 8 %) output mirrors. The two faces of the active element were antireflection coated for the wavelength 1064 nm. The pump radiation was focused by a lens into a spot 250 μm in diameter. As a selecting element, we used an intracavity Fabry–Perot etalon made of a YAG crystal in the form of a plane-parallel plate about 80 μm thick with reflecting coatings (reflection coefficient $R = 60$ %) on both faces.

Figure 2b shows the tuning curves for the lasers based on the *c*-cut $Nd:GdVO_4$, $Nd:YVO_4$, and $Nd:Gd_{0.7}Y_{0.3}VO_4$

crystals. In the case of the absorbed pump power $P_p = 5.4$ W, the wavelength of the Nd : $GdVO_4$ crystal was smoothly tuned within the range of 1062.3 – 1066.1 nm. At $P_p = 2.5$ W, we observed two separate nonoverlapping tuning ranges. In contrast, tuning in the *a*-cut Nd : $GdVO_4$ crystals was achieved only in the range of 1.2 nm around the wavelength 1063.2 nm. A similar tuning behaviour was observed for the *c*-cut yttrium and mixed vanadate crystals.

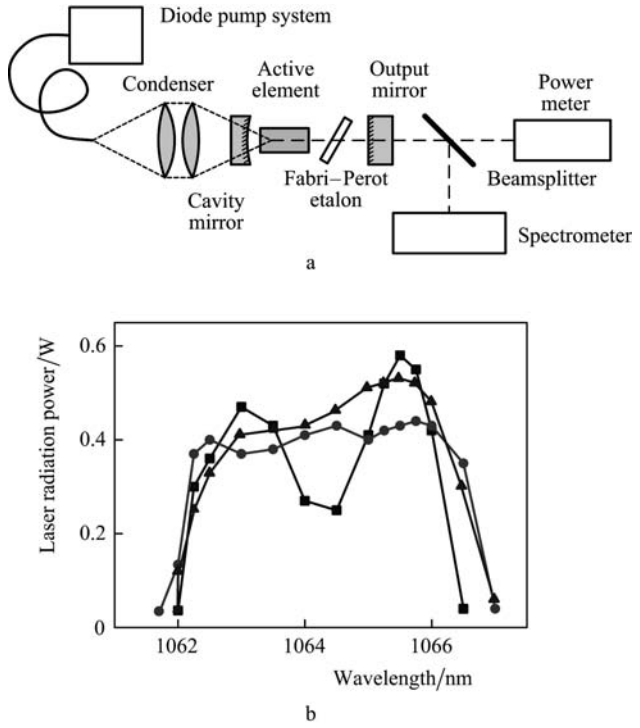


**Figure 2.** (a) Scheme of the frequency-tunable diode-pumped vanadate laser and (b) tuning curves for the *c*-cut (■) Nd : $GdVO_4$, (●) Nd : $YVO_4$, and (▲) Nd : $Gd_{0.7}Y_{0.3}VO_4$ lasers based on the $^4F_{3/2} - {}^4I_{9/2}$ transition.

When using a Lyot filter as a selecting element, we observed a stepwise tuning at wavelengths of 1063.2 and 1065.5 nm in the case of the Nd : $GdVO_4$ crystal and at 1063 and 1065.4 nm for the Nd : $Gd_{0.7}Y_{0.3}VO_4$ crystal. Similar stepwise tuning at three wavelengths occurred in the case of the Nd : $YVO_4$ crystal. However, to obtain stable two-frequency radiation, it is preferable to use the *c*-cut Nd : $GdVO_4$ crystal due to the more pronounced two-peak structure of the tuning curve and to close values of peak intensities in the luminescence spectra.

In this work, we for the first time proposed and realised a promising method of wavelength tuning for the *c*-cut Nd : $GdVO_4$ crystal. This crystal exhibits a pronounced dependence of the luminescence profile on the angle between the beam propagation and the *c* axis. With changing angular position of the *c*-cut crystal, the luminescence maximum shifts from one spectral peak to the other (see Fig. 1a). Thus, without using any additional selecting element, the rotation of the active element with respect to the cavity axis results in the lasing either at the wavelength 1063.2 nm or at 1065.5 nm. When the angular position of the active element was finely adjusted so that the emission intensities at these two wavelengths were equal, we obtained lasing simultaneously at 1063.2 and 1065.5 nm. However, this two-frequency regime was unstable and depended on the stability of the cavity, pumping, and the crystal temperature.

## 4. Method of two-frequency lasing

The principle used in this work to obtain two-frequency lasing is based on introducing additional selecting elements (spectrally selective losses) to equalise the cavity *Q*-factors in the two regions of the luminescence spectra. In the case of equal *Q*-factors at two neighbouring spectral lines, lasing occurs simultaneously at these two frequencies.

As selecting elements for this purpose we used:

(i) A Fabry – Perot etalon (a plane-parallel plate made of a ~100-μm-thick YAG crystal with reflecting coatings with $R = 60$ %),

(ii) a Lyot filter (single-stage with thicknesses of 0.57, 1.14, and 5.7 mm or three-stage in the form of crystalline quartz plates placed at the Brewster angle to the cavity axis),

(iii) a Brewster prism made of TF-5 glass.

It should be noted that the schemes of two-frequency lasers with a Lyot filter and a Brewster prism were proposed and experimentally realised in this work for the first time.

Below we describe the method of simultaneous two-frequency lasing on the example of a *c*-cut Nd : $GdVO_4$ crystal with a Lyot filter as a selecting element.

Figure 1a shows the luminescence spectrum of the *c*-cut Nd : $GdVO_4$ crystal. The spectrum contains two peaks at wavelengths $\lambda_1 = 1063.2$ and $\lambda_2 = 1065.5$ nm. The wavelength dependence of losses in the Lyot filter has a sinusoidal shape. Rotating the Lyot filter around its axis, we introduce losses in different spectral regions and thus change the cavity *Q*-factor $Q(\lambda)$ in these regions. At $Q(\lambda_1) < Q(\lambda_2)$, lasing occurs at wavelength $\lambda_2$, and at $Q(\lambda_1) > Q(\lambda_2)$ we obtain laser radiation at $\lambda_1$. A fine adjustment of the Lyot filter allows us to achieve identical intensities of radiation at these wavelengths. When the *Q*-factors become equal $[Q(\lambda_1) = Q(\lambda_2)]$, lasing occurs simultaneously at two wavelengths corresponding to the two peaks in the luminescence spectrum, i.e. at $\lambda_1$ and $\lambda_2$. Obviously, the difference between the wavelengths of generated radiation in the case of using the Lyot filter is determined only by the positions of two peaks in the luminescence spectrum of the crystal.

For the Fabry – Perot etalon, the wavelengths difference between the transmission maxima is determined by the interferometer free spectral range: $\lambda_1 - \lambda_2 = \lambda^2/(2nd)$, where *n* is the refractive index, *d* is the etalon thickness, and $\lambda = (\lambda_1 + \lambda_2)/2$. With changing the angle of inclination of the Fabry – Perot etalon to the beam axis, its transmission maxima shift with respect to the luminescence spectra and, when these maxima coincide with two regions in which the luminescence intensity is identical, we achieve the two-frequency lasing regime. In the case of using a Fabry – Perot etalon, the wavelength difference of the output radiation is determined only by the etalon free spectral range. In our experiments, we used Fabry – Perot etalons of different thickness, which lead to a change in the difference $\lambda_1 - \lambda_2$ from 1.3 to 3.9 nm. This will allow one to obtain frequency-tunable terahertz radiation in the future.

A Brewster prism causes spectral and spatial selection of radiation inside the cavity. By rotating the prism and choosing the cavity parameters, one can equalise the gain at two luminescence peaks and obtain lasing simultaneously at these two frequencies. The difference between these fre-

quencies is determined, similar to the case with a Lyot filter, only by the wavelengths corresponding to the two luminescence maxima of the $Nd:GdVO_4$ crystal.

The experiments showed that the lasers with a Brewster prism have the most stable parameters for two-frequency lasing, which is caused by the additional spatial selection of radiation over the active medium cross section.

The spectrum of laser radiation at two wavelengths (1063.2 and 1065.5 nm) generated by a $Nd:GdVO_4$ laser with a Lyot filter as a selecting element is shown in Fig. 3.

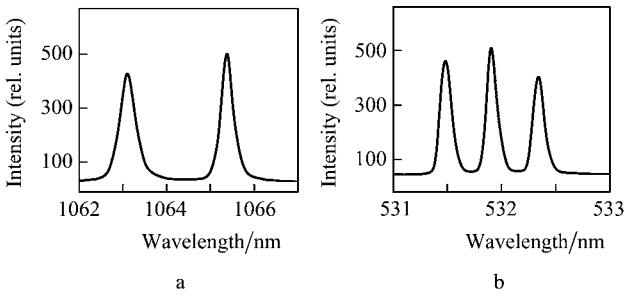


**Figure 3.** Spectra of (a) a two-frequency $Nd:GdVO_4$ laser and (b) of the second harmonic and sum-frequency generation.

The two-frequency lasing at the $^4F_{3/2}-{}^4I_{11/2}$ transition in $Nd:GdVO_4$ crystals was obtained in the cw regime, as well as in the acousto-optic *Q*-switched and active acousto-optic mode-locked regimes.

We used a *c*-cut active element $4\times4\times6$ mm in size. Both faces of the element were AR coated for a wavelength of 1604 nm. One of the faces was cut at an angle of 1.5°. The elements were fixed with the help of indium foil in copper blocks cooled by Peltier elements or water flow. The active element was pumped by a fibre-coupled (core diameter 200 μm, numerical aperture NA = 0.22) HLU30F200 (LIMO) laser diode array with the maximum output power of 30 W at a wavelength of 808 nm. The pump radiation was focused by a system of objectives, which allowed us to have the pump spot diameter from 150 to 400 μm in the crystal. We used a Z-fold cavity (Fig. 4).

The active element was placed close to the highly reflecting mirror through which it was pumped. The pump beam was focused in the active element into a spot ~350 μm in diameter. To eliminate the 'etalon effect', all the planes of intracavity optical elements were cut at the Brewster angle and the substrates were wedge-shaped. The Z-fold cavity consisted of a highly reflecting dielectric mirror, two spherical mirrors (curvature radius 100 mm), and a wedge-shaped (angle 1.5°) output mirror ($T = 5\,\%$, 10 %, and 25 %). To compensate the astigmatism of spherical mirrors, their axes were rotated at an angle of ~ 16° with respect to the cavity axis. As selecting elements for two-frequency lasing, we used a Fabry–Perot etalon, a Lyot filter, or a Brewster prism.

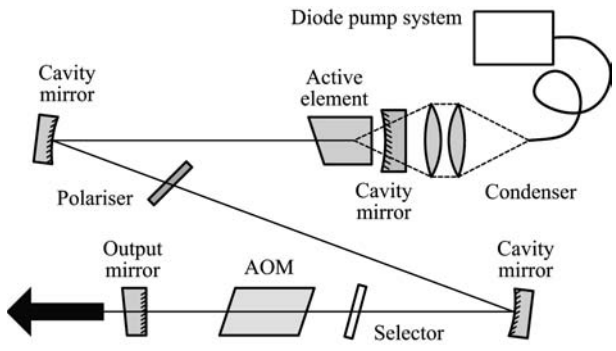


**Figure 4.** Scheme of the two-frequency laser.

The time parameters of nanosecond laser pulses were recorded with an LFD-2 fast avalanche photodiode and a Tektronix TDS3052 oscilloscope (transmission band 500 MHz). The duration of picosecond pulses was measured using a GPI Photoelectronics Dept. Mod. PN-01/s20 streak camera with a resolution of 1.7 ps.

The lasing threshold in the cw regime was 1.51 W, and the maximum output power reached 640 mW at the absorbed pump power 12 W.

For the *Q*-switched regime, we used an M3-321M acousto-optic modulator (AOM) controlled by a GSN 50-30I sinusoidal voltage generator with a high-frequency signal power up to 30 W. The laser operated in a repetitively pulsed regime with a pulse repetition rate of 5–15 kHz and a pulse duration of 40–60 ns. The maximum average output power reached 590 mW at a pulse repetition rate of 8 kHz.

To obtain the mode-locked regime, we placed an ML-202 AOM near the output mirror. The AOM was thermally stabilised with an accuracy of 0.1 °C using a Peltier microcooler. The AOM modulation frequency was 70 MHz, which corresponded to the geometric cavity length 1037 mm (or to the optical length 1071 mm), and the pulse repetition rate in this case was 140 MHz. The high-frequency signal power varied within 1.5–8 W. The cavity length was adjusted to the AOM frequency using a precision translation stage. At a pump power exceeding 3 W, we observed a stable train of laser pulses with an average output power of 340 mW at a pulse duration of 40–60 ps.

Figure 5 shows the dependences of the average output power of the two-frequency laser in cw, *Q*-switched, and mode-locked regimes.

To verify that the laser operates simultaneously at two wavelengths, we used the second harmonic generation in a KTP nonlinear crystal. After conversion of the two-frequency radiation corresponding to the two luminescence peaks at $\lambda_1 = 1063.0$ nm and $\lambda_2 = 1065.3$ nm, we recorded

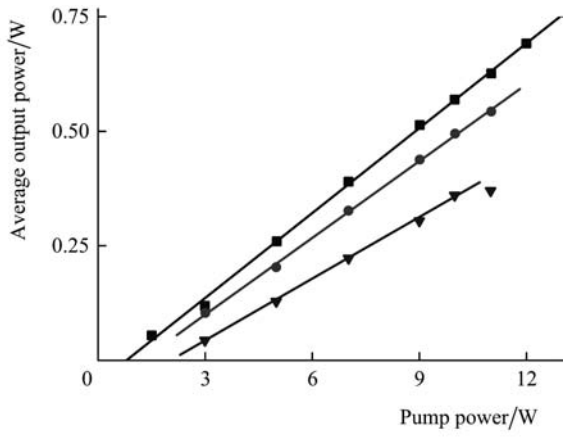


**Figure 5.** Average output power of the two-frequency $Nd:GdVO_4$ laser in the (■) cw, (●) nanosecond, and (▲) picosecond regimes.

three peaks of the second and summed harmonics with wavelengths $\lambda_1/2$, $\lambda_2/2$, and $(\lambda_1/2 + \lambda_2/2)/2$ (Fig. 3b). The peak at the summed frequency unambiguously indicates that lasing occurs simultaneously at two wavelengths both in the cw regime and in the *Q*-switched and mode-locked regimes.

## 5. Conclusions

It is experimentally shown that the total luminescence profile of *c*-cut yttrium, gadolinium, and mixed vanadate crystals is considerably wider than in the *a*-cut crystals and that the laser radiation wavelengths are tuned within 5.4 nm. Two-frequency laser schemes with the use of a Lyot filter, a Fabry–Perot etalon, and a Brewster prism as selecting elements are proposed and experimentally realised. A stable two-frequency lasing at the $^4F_{3/2} - {}^4I_{11/2}$ transition of the neodymium ion in the *c*-cut $Nd:GdVO_4$ crystals is obtained in the following regimes:

(i) cw regime (the maximum output power reached 640 mW at the absorbed pump power 12 W);

(ii) acousto-optic *Q*-switched regime (nanosecond region) (the laser generated pulsed-periodic radiation with a pulse repetition rate of 5–15 kHz, a pulse duration of 40–60 ns, and a maximum output power up to 590 mW at a pulse repetition rate 8 kHz);

(iii) active acousto-optic mode-locked regime (picosecond region) (a stable train of laser pulses with an average output power of 340 mW at a pulse duration of 40–60 ps was observed at a pump power exceeding 10 W).

***Acknowledgements.*** This work was partly supported by the Russian Foundation for Basic Research (Grant Nos 07-02-12109 and 09-02-00861-a).

## References

1. Smith P.R., Auston D.H., Nuss M.C. *IEEE J. Quantum Electron.*, **24**, 255 (1998).
2. Lui K.P., Hegmann F.A. *Appl. Phys. Lett.*, **78**, 3478 (2001).
3. Leitenstorfer A., Hunsche S., Shah J., Nuss M.C., Knox W.H. *Phys. Rev. B*, **61**, 16642 (2000).
4. Hunsche S., Koch M., Brener I., Nuss M.C. *Opt. Commun.*, **150**, 22 (1998).
5. Jeon T.-I., Grischkowsky D., Mukherjee A.K., Menon R. *Appl. Phys. Lett.*, **77**, 2452 (2000).
6. Mittleman D.M., Jacobsen R.H., Neelamani R., Braniuk R.G., Nuss M.C. *Appl. Phys. B*, **67**, 379 (1998).
7. Zandonella C. *Nature*, **424**, 721 (2003).
8. Willer U., Wilk R., Schippers W., Bottger S., Nodop D., Schossig T., Schade W., Mikulics M., Koch M., Walther M., Niemann H., Uttler B.G. *Appl. Phys. B*, **87**, 13 (2007).
9. Verghese S., McIntiosh K.A., Calawa S., Dinatale W.F., Duerr E.K., Molvar K.A. *Appl. Phys. Lett.*, **73**, 3824 (1998).
10. Lee Y.S., Meade T., Norris T.B., Galvanauskas A. *Appl. Phys. Lett.*, **78**, 3583 (2001).
11. Ding Y.J. *IEEE J. Sel. Top. Quantum Electron.*, **13**, 705 (2007).
12. Siebert K.J., Quast H., Leonhardt R., Löffler T., Thomson M., Bauer T., Roskos H., Czasch S. *Appl. Phys. Lett.*, **80**, 3003 (2002).
13. Breede M. et al. *Opt. Commun.*, **207**, 261 (2002).
14. Kleine-Ostmann T., Knobloch P., Koch M., Hoffmann S., Breede M., Hofmann M., Hen G., Pierz K., Sperling M., Donhuijsen K. *Electron. Lett.*, **37**, 1461 (2001).
15. Chen Y.F., Lan Y.P. *Appl. Phys. B*, **74**, 415 (2002).
16. Liu J., Yang J., He J. *Opt. Commun.*, **219**, 317 (2003).
17. Vlasov V.I., Garnov S.V., Zavertsev Yu.D., Zagumennyi A.I., Kutovoi S.A., Sirotkin A.A., Shcherbakov I.A. *Kvantovaya Elektron.*, **37** (10), 938 (2007) [*Quantum Electron.*, **37** (10), 938 (2007)].